



LJMU Research Online

Li, R, Zhang, X, Jiang, L, Yang, Z and Guo, W

An adaptive heuristic algorithm based on reinforcement learning for ship scheduling optimization problem

<http://researchonline.ljmu.ac.uk/id/eprint/18040/>

Article

Citation (please note it is advisable to refer to the publisher's version if you intend to cite from this work)

Li, R, Zhang, X, Jiang, L, Yang, Z and Guo, W (2022) An adaptive heuristic algorithm based on reinforcement learning for ship scheduling optimization problem. Ocean and Coastal Management, 230. pp. 1-15. ISSN 0964-5691

LJMU has developed **LJMU Research Online** for users to access the research output of the University more effectively. Copyright © and Moral Rights for the papers on this site are retained by the individual authors and/or other copyright owners. Users may download and/or print one copy of any article(s) in LJMU Research Online to facilitate their private study or for non-commercial research. You may not engage in further distribution of the material or use it for any profit-making activities or any commercial gain.

The version presented here may differ from the published version or from the version of the record. Please see the repository URL above for details on accessing the published version and note that access may require a subscription.

For more information please contact researchonline@ljmu.ac.uk

<http://researchonline.ljmu.ac.uk/>

An adaptive heuristic algorithm based on reinforcement learning for ship scheduling optimization

Runfo Li ^a, Xinyu Zhang ^{a,b,*}, Lingling Jiang ^c, Wenqiang Guo ^a

^a Maritime Intelligent Transportation Research Team, Navigation College, Dalian Maritime University, Dalian 116026, China

^b Shenzhen Research Institute of Dalian Maritime University, Shenzhen 116026, China

^c College of Environmental Sciences and Engineering, Dalian Maritime University, Dalian, 116026, China

Abstract: Due to the development of ship size and the traffic increase in port, ships having long turnaround time in port often result in port congestion, which seriously affects the efficiency and environmental sustainability of ship navigation. It has been evident that effective ship scheduling presents a solution of fundamental and strategic importance to port congestion. In this paper, a mixed-integer linear programming mathematical model is developed to realise the optimization of ship scheduling in port to minimize the total time spent by ships in port. Its methodological novelty is gained by an innovative adaptive genetic simulated annealing algorithm based on a reinforcement learning algorithm (GSAA-RL) to support the developed mathematical model, in which the genetic algorithm is considered as the basic optimization algorithm, and Q-learning with a unique property of selecting suitable parameters dynamically is developed to adjust the parameters of crossover and mutation to improve the search ability of the algorithm. Meanwhile, the dynamic parameter turning process is formulated into a Markov decision process (MDP) model with well defining the state, action, and reward function in GSAA-RL. Specifically, the state sets are proposed by analyzing the key factors affecting the scheduling efficiency and a new reward mechanism that can reduce the objective value significantly based on the quality of selected parameters is designed. The annealing operation is performed on some excellent individuals to further expand the search scope. Simulation experiments demonstrate that the proposed GSAA-RL algorithm can significantly shorten the total time spent by ships in port compared to existing approaches. The findings hence make contributions to ship owners for their improved operation efficiency and to port operators/authorities for the reduction of port congestions.

Keywords: Q-learning; Adaptive genetic simulated annealing algorithm; Ship traffic scheduling; Maritime transportation.

1. Introduction

Since the new century, we have witnessed the fast growth of the maritime industry to respond to the tremendous development of global trade. The volume of world maritime trade increased from 8.4 billion tons in 2010 to 10.6 billion tons in 2020 [1]. As an essential part of maritime transportation, ports undertake the vital mission of radiating and driving the economic development of coastal areas, hence receiving widespread attention from academia and industry. However, the rapid increases of both ship size and traffic in ports have posed ship delays and traffic congestion in port, leading to a significant increase in operating costs and a serious decline in service quality. It is extremely costly to alter a port layout and infrastructure after its initial establishment, rationally organizing and dispatching the inbound and outbound ships is deemed to be a realistic and effective solution to alleviation of traffic congestion and ships delay [2].

According to the surveys of port, it is found that the current ships entering and leaving the port

* Corresponding author.

E-mail addresses: 15352856102@163.com (Runfo Li), zhangxy@dlnu.edu.cn (Xinyu Zhang).

41 are mainly scheduled by VTS staff based on human experience under the guidance of port navigation
42 rules. Obviously, this method takes more human factors into consideration and lacks a certain
43 theoretical guidance. It is difficult to ensure the efficiency and rationality of scheduling, which further
44 leads to the unnecessary waiting time of ships entering and leaving the port. Therefore, for port
45 managers and ship owners, it is urgent to shift the current scheduling paradigm towards a new and
46 efficient scheduling method which enables the optimal scheduling even under a complex traffic
47 circumstance.

48 In light of this practical demand, many scholars have proposed different types of methods to study
49 the complex problem of ship scheduling. Table 1 presents some classical methods in the relevant area.
50 Some scholars have proposed precise approaches to provide optimal solutions. Specifically, it includes
51 a branch and bound algorithm [3], a column generation algorithm [2,4], and a lagrangian relaxation
52 algorithm [5]. However, the precise algorithms take long computational time, and it is difficult to
53 obtain a global optimal solution even for small-scale calculation examples. Therefore, heuristic
54 methods are proposed to solve the problem, including a simulated annealing multi-population genetic
55 algorithm [6], a simulated annealing algorithm [7,8], and a hybrid algorithm combining heuristic rules
56 and simulated annealing algorithm [9], a meta-heuristic algorithm [10,11,12], a non-dominated sorting
57 genetic algorithm [13,14], a genetic algorithm [16,17,18], a tabu search algorithm [19], a large
58 neighborhood search algorithm [15]. Although showing much attractiveness in ship scheduling
59 optimization, previous studies still revealed some concerns of which the theoretical implications have
60 yet been well addressed in the existing literature. Among the significant ones is the determination of
61 the optimization algorithm parameters which is crucial in terms of the improvement of solution quality.

62 With the rapid development of machine learning technologies in recent years, a few scholars have
63 put effort on reinforcement learning to adaptively adjust the parameters of heuristic algorithms.
64 Compared with the limitations of heuristic algorithms that directly give specific parameters in a
65 specified solution space, reinforcement learning has the advantage of being able to select suitable
66 parameters by revealing the internal structure of the population [20,21]. Shahrabi et al. [22] proposed
67 to use a Q-learning algorithm in reinforcement learning to improve the performance of the variable
68 neighborhood search algorithm for the dynamic workshop scheduling problem of machine failure. In
69 order to obtain a feasible shop scheduling sequence in a limited period, Cao et al. [23] proposed a
70 knowledge-based cuckoo search algorithm, which incorporated the Sarsa algorithm into the cuckoo
71 algorithm to effectively improve the cuckoo algorithm's performance. Pettinger et al. [24] proposed a
72 hybrid system for the traveling salesman problem. The system used Q learning algorithm to estimate
73 the state-action value, which is used to realize the advanced adaptive control of the genetic algorithm.
74 Based on the reserve selection mechanism, Chen et al. [25] proposed an optimal reserve scale learning
75 method based on reinforcement learning technologies and conducted experimental verification. The
76 verification results proved that the proposed algorithm is effective in finding the optimal reserve scale.
77 Meng et al. [26] proposed an improved reinforcement learning-based dynamic priority algorithm for
78 parameter optimization to solve the problem of selecting scheduling performance index in a dynamic
79 priority algorithm. The experimental results demonstrated that the improved reinforcement learning
80 algorithm can not only optimize the weight parameters but also reduce the deadline error rate.

81 Although the methods of adjusting and optimizing heuristic algorithm parameters by
82 reinforcement learning have been applied in the fields of job shop scheduling, product manufacturing,
83 and power systems, there is little evidence to the authors' best knowledge that that the reinforcement
84 learning has been used to optimise heuristic algorithm parameters in maritime transport and less in

85 ship scheduling for the purpose of shortening the total time of ships for entering and leaving the port
 86 The key to using reinforcement learning to adjust the parameters of the heuristic algorithm lies in the
 87 setting of the Markov decision process (MDP) adjustment parameter model (e.g. state sets, action sets
 88 and reward functions). The MDP model constructed in other fields is obviously not applicable in the
 89 shipping field, due to its unique characteristics.

90 In this paper, an adaptive genetic simulated annealing algorithm based on a reinforcement
 91 learning algorithm (GSAA-RL) is designed. In GSAA-RL, the dynamic parameter turning process is
 92 formulated into a MDP model with well defining the state, action, and reward function. Specifically,
 93 by analyzing the key factors affecting ship scheduling, a state set that conforms to the realistic situation
 94 of ships entering and leaving the port is divided. A new reward mechanism that can significantly reduce
 95 the objective value based on the quality of selected parameters is developed to improve the learning
 96 efficiency of Q-learning, and reduce the number of iterations of the GSAA-RL algorithm. In addition,
 97 the annealing operation is performed on some excellent individuals to further expand the search scope.
 98 The proposed solution algorithm is evaluated and benchmarked against the First Come First Service
 99 (FCFS) strategy, CPLEX solver, genetic algorithm (GA), and genetic simulated annealing algorithm
 100 (GSAA), which have been frequently used as the norms for the ship scheduling literature.

101 The main contributions of this paper are summarised as follows:

102 First, a new GSAA-RL algorithm is proposed based on the characteristics of the specific shipping
 103 scheduling problem to solve a mixed-integer linear programming (MILP) model. Compared to the
 104 existing methods, the algorithm is new in a sense that it aids more reduction of the total time spent of
 105 ships entering and leaving the port.

106 Second, an MDP model with a property of turning parameter dynamically is constructed, where
 107 the state sets for the ship scheduling optimization problem are proposed through the analysis of the
 108 key factors affecting the scheduling efficiency. It is more consistent with the real situation to be
 109 modelled.

110 Third, a new reward mechanism is designed to effectively minimize the total time spent by ships
 111 in port based on the quality of selected parameters. It significantly improves the learning efficiency of
 112 Q-learning and reduces the number of GSAA-RL algorithm iterations.

113 The remainder of this paper is organized as follows. Section 2 describes the problem statement
 114 and modeling. Section 3 presents the details for the implementation of the GSAA-RL algorithm.
 115 Computational experiments are conducted in Section 4. Section 5 concludes the paper and provides
 116 the possible directions for future studies.

117 **Table 1**

118 Summary of methods for solving ship traffic scheduling problems.

AUTHORS	OM		
	EM	HM	RL
Jia et al. 2019	CG		
Liu et al. 2021	CG		
Li et al. 2019	LR		
Wu et al. 2021	BB		
Lalla et al. 2016		SA	
Pei et al. 2018		SA	
Zhang et al. 2016		GA+SA	
Zheng et al. 2018		SA+HR	

Meisel et al. 2019	MHM	
Andersen et al. 2021	MHM	
Soroush et al. 2020	MHM	
Zhang et al. 2020	GA	
Liu et al. 2021	GA	
Zhang et al. 2018	NSGA-II	
Zhang et al. 2019	NSGA-II	
Li et al. 2021	NSGA-II+TS	
Liu et al. 2021	LNSA	
This study	GA+SA	RL

119 OM: optimization method; EM: exact method; HM: heuristic method; RL: reinforcement learning;
120 CG: column generation algorithm; BB: branch and bound algorithm; LR: lagrangian relaxation
121 algorithm; SA: simulated annealing algorithm; GA: genetic algorithm; HR: heuristic rule; MHM: meta
122 heuristic method; TS: tabu search; LNSA: large neighborhood search algorithm; NSGA-II: non-
123 dominated sorting genetic algorithm II.

124 2. Problem statement and modeling

125 Ship operation in port is a complex process, involving a safe and feasible scheduling plan to
126 anticipate and avoid ships facing urgent situations in the nearby waters (e.g. channels) in advance. The
127 key to ship scheduling in one-way navigable ports is to reasonably arrange the sequence and time of
128 ships entering and/or leaving the ports for ensuring the ships' safety and improving their navigation
129 efficiency.

130 The ship scheduling problem in this paper can be described as follows: under the condition that
131 the pre-docking berths of ships are known, all the ships expected to arrive and depart from the port in
132 a fixed planning period are taken as the research objects, focusing on the avoidance of realistic
133 constraints such as risky encounters and tidal time windows. It takes into account various ship driving
134 service rules, while minimizing the total waiting time of all arriving ships as the optimization goal,
135 and giving the best time for each ship to enter and leave the port. It should be noted that the basic ship
136 data used in the ship scheduling model established in this paper are deterministic, leaving the effect of
137 uncertainty in data against the relevant factors on ship scheduling to be separately presented.

138 2.1. Model assumptions

139 There are many complex factors that affect the ship traffic scheduling in port. The key factors are
140 extracted with the following assumptions rationally made in this paper.

141 (1) For the in-wharf ships, the application time refers to the time when they apply to enter the
142 port; For the out-wharf ships, the application time refers to the time when they apply for leaving the
143 berth;

144 (2) The berths by incoming ships have been allocated in advance;

145 (3) The number of pilots is sufficient;

146 (4) During the ship scheduling process, the influence of weather, accidents, and other possible
147 disturbances on the ship is not taken into account;

148 (5) All ships entering and leaving the port are in the same position away from the channel;

149 (6) When the ship applies for entering and leaving the port, the pilot and tugboat have been
150 allocated and ready to use.

151

Table 2

152

The main components of the proposed mathematical model.

Sets and parameters	
V^{in}	set of all inbound ships, $i \in \{1, 2, \dots, V^{in} \}$
V^{out}	set of all outbound ships, $i \in \{1, 2, \dots, V^{out} \}$
V	set of all ships, $i \in \{1, 2, \dots, V \}$, $V = V^{in} \cup V^{out}$
B	set of all berths, $i \in \{1, 2, \dots, B \}$
d_{1i}	the distance for ship i from the entry of the channel to its anchor, $i \in V$
d_2	the distance from the entrance to the exit of the channel
d_{3i}	the distance for ship i from the exit of the channel to its berth, $i \in V$
v_i	the speed of ship i , $i \in V$
M	a sufficiently large positive integer
Decision Variables	
t_{si}	the starting time of ship i needs to enter or leave the port by the tide, $i \in V$
t_{ei}	the ending time of ship i needs to enter or leave the port by the tide, $i \in V$
t_i^{a-in}	the application time of ship i , $i \in V^{in}$
$t_i^{a'-in}$	the adjusted application time of ship i , $i \in V^{in}$
t_{ib}^{s-in}	the beginning scheduling time of ship i which will berth in berth b when entering the port, $i \in V^{in}$, $b \in B$
t_{ib}^{1-in}	the time when the ship i allocated to berth b approaches the channel, $i \in V^{in}$, $b \in B$
t_{ib}^{2-in}	the time when the ship i associated to berth b leaves the channel, $i \in V^{in}$, $b \in B$
t_{ib}^{f-in}	the time when the ship $i \in V^{in}$ finishes scheduling, which is the time of arriving at berth b , $i \in V^{in}$, $b \in B$
t_i^{a-out}	the application time of ship i , $i \in V^{out}$
$t_i^{a'-out}$	the adjusted application time of ship i , $i \in V^{out}$
t_{ib}^{s-out}	the beginning scheduling time when ship i in berth b leaves the port, $i \in V^{out}$, $b \in B$
t_{ib}^{1-out}	the time when the ship i allocated in berth b approaches the channel, $i \in V^{out}$, $b \in B$
t_{ib}^{f-out}	the time when the ship i allocated in berth b finished scheduling, $i \in V^{out}$, $b \in B$
g_1	a minimum safe time interval is required for the ship to avoid an overtaking situation
g_2	a minimum safe time interval is required for the ship to avoid a cross-encounter or confrontation situation
T_i	binary, equal to 1 if ship i needs to take tide to the port, and 0 otherwise, $i \in V$
R_{ij}	binary, equal to 1 if ship j is scheduled after ship i when entering, $i, j \in V^{in}$
Z_{ij}	binary, equal to 1 if ship j is scheduled after ship i when leaving, $i, j \in V^{out}$
IO_i	binary, equal to 1 if ship i is entering the port, and 0 otherwise, $i \in V$

153

2.2. Model building

154

According to the sets, parameters, and decision variables shown in Table 2 and the above assumptions, the one-way ship traffic scheduling problem is modeled as an MILP model as follows.

155

156

Minimize

$$157 \quad OS = \sum_{i \in V^{in}} \sum_{b \in B} (t_{ib}^{s-in} - t_i^{a-in}) + \sum_{i \in V^{out}} \sum_{b \in B} (t_{ib}^{s-out} - t_{ib}^{a-out}) \quad (1)$$

158 Subject to

$$159 \quad t_i^{1-in} = t_i^{s-in} + \frac{d_{1i}}{v_i}, \forall i \in V^{in} \quad (2)$$

$$160 \quad t_i^{2-in} = t_i^{1-in} + \frac{d_2}{v_i}, \forall i \in V^{in} \quad (3)$$

$$161 \quad t_i^{f-in} = t_i^{2-in} + \frac{d_{3i}}{v_i}, \forall i \in V^{in} \quad (4)$$

$$162 \quad t_i^{1-out} = t_i^{s-out} + \frac{d_{3i}}{v_i}, \forall i \in V^{out} \quad (5)$$

$$163 \quad t_i^{f-out} = t_i^{1-out} + \frac{d_2}{v_i}, \forall i \in V^{out} \quad (6)$$

$$164 \quad T_i = 1 \rightarrow t_i^{a-in} = \begin{cases} t_{si}, t_i^{a-in} \leq t_{si} \\ t_i^{a-in}, t_{si} \leq t_i^{a-in} \leq t_{ei} \end{cases}, \forall i \in V^{in} \quad (7)$$

$$165 \quad T_i = 1 \rightarrow t_i^{a-out} = \begin{cases} t_{si}, t_i^{a-out} \leq t_{si} \\ t_i^{a-out}, t_{si} \leq t_i^{a-out} \leq t_{ei} \end{cases}, \forall i \in V^{out} \quad (8)$$

$$166 \quad t_i^{s-in} \geq \begin{cases} t_i^{a-in}, T_i = 1 \\ t_i^{a-in}, T_i = 0 \end{cases}, \forall i \in V^{in} \quad (9)$$

$$167 \quad t_i^{s-out} \geq \begin{cases} t_i^{a-out}, t_i = 1 \\ t_i^{a-out}, t_i = 0 \end{cases}, \forall i \in V^{out} \quad (10)$$

$$168 \quad t_{ib}^{1-in} - t_{jb}^{1-in} + g_1 \leq M(1 - R_{ij}), \forall i, j \in V^{in}, \forall b \in B \quad (11)$$

$$169 \quad t_{ib}^{1-out} - t_{jb}^{1-out} + g_1 \leq M(1 - Z_{ij}), \forall i, j \in V^{out}, \forall b \in B \quad (12)$$

$$170 \quad \frac{t_{ib}^{s-out} + \frac{d_{1j}}{v_j} - (t_{ib}^{s-in} + \frac{d_2}{v_i})}{g_2} - \frac{\hat{I}_i - \hat{I}_j}{g_2} \geq 0, i \in V^{in}, j \in V^{out}, b \in B \quad (13)$$

$$171 \quad \frac{t_{ib}^{s-in} + \frac{d_{1j}}{v_j} - (t_{ib}^{s-out} + \frac{d_2}{v_i} + \frac{d_{3i}}{v_i})}{g_2} - \frac{\hat{I}_i - \hat{I}_j}{g_2} \geq 0, j \in V^{in}, i \in V^{out}, b \in B \quad (14)$$

$$172 \quad IO_i \in \{0, 1\}, \forall i \in V \quad (15)$$

$$173 \quad T_i \in \{0, 1\}, \forall i \in V \quad (16)$$

$$174 \quad R_{ij} \in \{0, 1\}, i, j \in V^{in} \quad (17)$$

$$175 \quad Z_{ij} \in \{0, 1\}, i, j \in V^{out} \quad (18)$$

176 The objective function (1) aims to minimize the total time spent by ships entering and leaving the
177 port, it includes sailing time and waiting time of all ships in port. Constraints (2)-(4) state the sailing
178 continuity of in-wharf ships. The time at which the ship sails to the entrance of the channel, the exit
179 of the channel and the berth at which it is berthed can be determined in turn. Constraints (5)-(6)
180 guarantee the sailing continuity of out-wharf ships. The time when the ship sails to the exit of the
181 channel and the entrance to the channel can be determined in turn. Constraints (7)-(8) ensure that the
182 ship taking a tide adjusts the application time to enter or leave the port. Constraints (9)-(10) state ship
183 can begin scheduling. Constraints (11)-(12) guarantee that a certain safety clearance should be
184 maintained between ships in the same direction and Constraints (13)-(14) ensure that ships in different
185 directions should maintain a safe clearance. Constraints (15)-(18) specify binary variables.

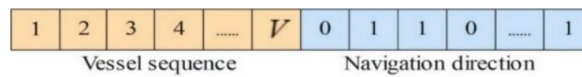
186 **3. Adaptive genetic simulated annealing algorithm based on**
187 **reinforcement learning (GSAA-RL)**

188 *3.1. Genetic simulated annealing algorithm*

189 Because the ship traffic scheduling problem belongs to a combinatorial optimization problem, it
190 is difficult to enumerate all the solutions by an enumeration method. Therefore, the optimization
191 algorithm is required to have high computational efficiency. Genetic algorithm is widely used to solve
192 combinatorial optimization problems due to their strong global searching ability and short computing
193 time. However, the traditional genetic algorithm has the disadvantage of local convergence, while the
194 simulated annealing algorithm has a strong local search ability [27] to further expand the search scope
195 of solutions. A simulated annealing algorithm is first introduced in this paper to accept a worse solution
196 with a certain probability.

197 *3.1.1. Chromosome representation and population initialization*

198 This process of generating a chromosome is regarded as chromosome initialization. In this paper,
199 a chromosome includes two layers, namely ship number and navigation direction respectively. An
200 example of a chromosome is shown in Fig. 1 and the population can be initialized according to the
201 number of individuals $NIND$.



202 **Fig. 1.** An example of a chromosome
203

204 *3.1.2. Genetic operations*

205 This paper selects the objective function of the total time spent by ships entering and leaving the
206 port as the fitness function (the first and fourth rows in Algorithm 1). According to the fitness function,
207 the regenerated individuals are selected. The selection strategy in this paper adopts stochastic universal
208 selection (line 9 in Algorithm 1), with the probability of $GGAP$ selecting some individuals with higher
209 fitness value from the parent as the offspring. After completing the selection operation, the selected
210 excellent individuals are paired and crossed. A single-point crossover is used for the crossover
211 operation (line 10 in Algorithm 1). Mutation operation plays an important role in improving the local
212 search ability of the genetic algorithm, and it is also an important step to generate new individuals,. In
213 the process of mutation operation, the genes of individuals in the population are randomly changed
214 according to a certain probability. The reverse mutation is used to carry out mutation operation (line
215 11 in Algorithm 1).

216 *3.1.3. Repair operation*

217 The repair operation is mainly to repair the illegal chromosomes generated by some genetic
218 operations. A ship i is about to dock at a berth m and another ship i is loading and unloading cargo on
219 the berth m , the ship i can only be scheduled after the ship j has loaded and unloaded the cargo.
220 However, after the initial chromosome has performed a series of genetic operations, the ship i may be
221 scheduled earlier than the ship j . Therefore, it is necessary to design a repair operation to repair illegal
222 chromosomes, that is, to readjust the order of ships entering and leaving the port. The repair method
223 is mainly to first identify the situation where two ships entering and leaving the port are served by a
224 berth at the same time, and then determine the scheduling order of the two ships. If ship i has priority

225 over ship j , then the gene positions corresponding to the two ships in the chromosome are exchanged.
 226 Otherwise, it means that the chromosome is feasible and there is no need to repair it.

227 3.1.4. Simulated annealing operation

228 When a certain number of new individuals are generated after genetic and repair operations, an
 229 annealing operation is used to determine whether the new individual should replace the old one. The
 230 Monte Carlo criterion in the simulated annealing algorithm is defined as follows.

$$231 \quad P = \begin{cases} 1, & y_2(x) < y_1(x) \\ e^{\frac{-(y_2(x)-y_1(x))}{T}}, & y_2(x) \geq y_1(x) \end{cases} \quad (17)$$

232 Here, it is assumed that $y_2(x)$ is the target value of the new individual and $y_1(x)$ is the target value of
 233 the old individual. If the target value of the new individual is smaller than that of the old one, the new
 234 individual will replace the old; otherwise, the new individual is accepted with probability $e^{\frac{-(y_2(x)-y_1(x))}{T}}$.

235 If $T > T_{end}$, the temperature is lowered through $T = q * T$ until the algorithm terminates.

236 3.2. MDP model construction

237 Q-learning is one of the most effective value-based RL algorithms. The construction of the MDP
 238 is regarded as the most important step in Q-learning [30]. The MDP can generally be described by four
 239 elements: state set S , action set A , reward function R , and strategy function π . In addition, the Q
 240 table is updated in Q-learning based on the comprehensive consideration of the experience state, the
 241 selected behavior, and the reward obtained by the agent, the Q table updated is performed by the
 242 following formula.

$$243 \quad Q(s_t, a_t) \leftarrow Q(s_t, a_t) + \alpha [r_t + \gamma \max_a Q(s_{t+1}, a_{t+1}) - Q(s_t, a_t)] \quad (18)$$

244 $Q(s_t, a_t)$ is the Q value after the agent performs a_t ; r_t is the instant reward; α is learning rate; γ
 245 is discount rate; $\max_a Q(s_{t+1}, a_{t+1})$ is when the agent is in the state s_{t+1} , after executing the action
 246 a_{t+1} , it expects to get the maximum Q value.

247 3.2.1. Design of state sets

248 In GSAA-RL, two key factors that affect the ship scheduling efficiency are selected to define the
 249 state sets. Through the comprehensive analysis of the in-wharf and out-wharf process, the number of
 250 ships (n) and the average total time spent by in port (AOS) are finally selected as the main factors. In
 251 order to limit the AOS value calculated in each generation to a certain range, we normalize it to
 252 eliminate the adverse effects caused by singular value. AOS' represents the average total time of
 253 entering and leaving the port normalized by the average total time spent by entering and leaving the
 254 port of the first generation population. AOS' can be calculated by the formula (19). Table 3 is the 27
 255 state sets finally divided through multiple experiments.

$$256 \quad AOS' = \frac{\sum_{i=1}^N Fit(x_i^t)}{N} \bigg/ \frac{\sum_{i=1}^N Fit(x_i^1)}{N} \quad (19)$$

257 Where $Fit(x_i^t)$ represents the fitness function of the i -th individual in the t -th iteration, $Fit(x_i^1)$

258 represents the fitness function of the i -th individual in the first iteration, and N is the number of
 259 individuals in the population.

260 **Table 3**

261 Definition of state sets.

State	ship number(n)	Average total time spent by ships in port (AOS')
s_1	$2 \leq n \leq 10$	$0.8 \leq \text{AOS}' \leq 0.85$
s_2	$2 \leq n \leq 10$	$0.85 \leq \text{AOS}' \leq 0.9$
s_3	$2 \leq n \leq 10$	$0.9 \leq \text{AOS}' \leq 0.95$
s_4	$2 \leq n \leq 10$	$0.95 \leq \text{AOS}' \leq 1.0$
s_5	$2 \leq n \leq 10$	$1.0 \leq \text{AOS}' \leq 1.05$
s_6	$2 \leq n \leq 10$	$1.05 \leq \text{AOS}' \leq 1.10$
s_7	$2 \leq n \leq 10$	$1.10 \leq \text{AOS}' \leq 1.15$
s_8	$2 \leq n \leq 10$	$1.15 \leq \text{AOS}' \leq 1.20$
s_9	$2 \leq n \leq 10$	$1.20 \leq \text{AOS}' \leq 1.25$
s_{10}	$11 \leq n \leq 19$	$0.8 \leq \text{AOS}' \leq 0.85$
s_{11}	$11 \leq n \leq 19$	$0.85 \leq \text{AOS}' \leq 0.9$
s_{12}	$11 \leq n \leq 19$	$0.9 \leq \text{AOS}' \leq 0.95$
s_{13}	$11 \leq n \leq 19$	$0.95 \leq \text{AOS}' \leq 1.0$
s_{14}	$11 \leq n \leq 19$	$1.0 \leq \text{AOS}' \leq 1.05$
s_{15}	$11 \leq n \leq 19$	$1.05 \leq \text{AOS}' \leq 1.10$
s_{16}	$11 \leq n \leq 19$	$1.10 \leq \text{AOS}' \leq 1.15$
s_{17}	$11 \leq n \leq 19$	$1.15 \leq \text{AOS}' \leq 1.20$
s_{18}	$11 \leq n \leq 19$	$1.20 \leq \text{AOS}' \leq 1.25$
s_{19}	$n \geq 20$	$0.8 \leq \text{AOS}' \leq 0.85$
s_{20}	$n \geq 20$	$0.85 \leq \text{AOS}' \leq 0.9$
s_{21}	$n \geq 20$	$0.9 \leq \text{AOS}' \leq 0.95$
s_{22}	$n \geq 20$	$0.95 \leq \text{AOS}' \leq 1.0$
s_{23}	$n \geq 20$	$1.0 \leq \text{AOS}' \leq 1.05$
s_{24}	$n \geq 20$	$1.05 \leq \text{AOS}' \leq 1.10$
s_{25}	$n \geq 20$	$1.10 \leq \text{AOS}' \leq 1.15$
s_{26}	$n \geq 20$	$1.15 \leq \text{AOS}' \leq 1.20$

262 3.2.2. Design of action sets and reward functions

263 During each iteration, the agent will choose different actions to get the appropriate crossover and
 264 mutation probabilities. For the crossover probability, we usually take the value from 0.4 to 0.9. The
 265 paper divides it into 10 intervals and the interval value is 0.05. As shown in Table 4. For the mutation
 266 probability, the value is usually from 0.01 to 0.21, which is divided into 10 intervals and the interval
 267 value is taken as 0.02, as shown in Table 5. For example, when an action a_1 is selected from action
 268 sets Pc , Pc is randomly selected from 0.4 to 0.46; Similarly, when an action a_2 is selected from
 269 action sets Pm , Pm is also randomly selected from 0.01 to 0.03. Next, the reward functions of
 270 crossover and mutation probabilities should be designed to evaluate whether the selection of their
 271 values is reasonable. Different reward functions may have different results under the same algorithm
 272 [28]. The setting of reward functions determines the convergence speed and efficiency of the algorithm.
 273 Chen et al. [29] set the following reward functions to evaluate the crossover and mutation probabilities
 274 in each iteration. They are defined as follows, respectively.

$$275 R_{crossover} = \frac{Fit_{best}(x_i^t) - Fit_{best}(x_i^{t-1})}{Fit_{best}(x_i^{t-1})} \quad (20)$$

$$276 R_{mutation} = \frac{\sum_{i=1}^N Fit(x_i^t) - \sum_{i=1}^N Fit(x_i^{t-1})}{\sum_{i=1}^N Fit(x_i^{t-1})} \quad (21)$$

277 Here, $Fit_{best}(x_i^t)$ represents the minimum fitness value of the i -th individual in the t -th generation,
 278 and $Fit_{best}(x_i^1)$ represents the minimum fitness value of the i -th individual in the first generation. But
 279 in the process of finding the target state, we must not only consider the situation of $Fit_{best}(x_i^t) < Fit_{best}(x_i^{t-1})$
 280 and $\sum_{i=1}^N Fit(x_i^t) / N < \sum_{i=1}^N Fit(x_i^{t-1}) / N$, but for the situation $Fit_{best}(x_i^t) \geq Fit_{best}(x_i^{t-1})$ and
 281 $\sum_{i=1}^N Fit(x_i^t) / N \geq \sum_{i=1}^N Fit(x_i^{t-1}) / N$ that appears in each iteration, the agent must be punished and given
 282 a negative reward value to force its state to change towards a good trend. Therefore, the following
 283 improved segmented reward functions are generated in the paper.

$$284 R_{crossover} = \begin{cases} 1, & Fit_{best}(x_i^t) < Fit_{best}(x_i^{t-1}) \\ -1, & Fit_{best}(x_i^t) \geq Fit_{best}(x_i^{t-1}) \end{cases} \quad (22)$$

$$285 R_{mutation} = \begin{cases} 1, & \frac{\sum_{i=1}^N Fit(x_i^t) - \sum_{i=1}^N Fit(x_i^{t-1})}{\sum_{i=1}^N Fit(x_i^{t-1})} < 0 \\ -1, & \frac{\sum_{i=1}^N Fit(x_i^t) - \sum_{i=1}^N Fit(x_i^{t-1})}{\sum_{i=1}^N Fit(x_i^{t-1})} > 0 \end{cases} \quad (23)$$

286 **Table 4**

287 Definition of action sets Pc .

Action	Range of parameter Pc
a_1	$0.4 \leq Pc \leq 0.45$

a_2	$0.45 \leq Pc \leq 0.50$
a_3	$0.50 \leq Pc \leq 0.55$
a_4	$0.55 \leq Pc \leq 0.60$
a_5	$0.60 \leq Pc \leq 0.65$
a_6	$0.65 \leq Pc \leq 0.70$
a_7	$0.70 \leq Pc \leq 0.75$
a_8	$0.75 \leq Pc \leq 0.80$
a_9	$0.80 \leq Pc \leq 0.85$
a_{10}	$0.85 \leq Pc \leq 0.90$

288 **Table 5**
289 Definition of action sets Pm .

Action	Range of parameter Pm
a_1	$0.01 \leq Pm \leq 0.03$
a_2	$0.03 \leq Pm \leq 0.05$
a_3	$0.05 \leq Pm \leq 0.07$
a_4	$0.07 \leq Pm \leq 0.09$
a_5	$0.09 \leq Pm \leq 0.11$
a_6	$0.11 \leq Pm \leq 0.13$
a_7	$0.13 \leq Pm \leq 0.15$
a_8	$0.15 \leq Pm \leq 0.17$
a_9	$0.17 \leq Pm \leq 0.19$
a_{10}	$0.19 \leq Pm \leq 0.21$

290 *3.2.3. Action selection strategy*

291 This paper selects the ε -greedy strategy of reinforcement learning as the action selection
292 strategy. The strategy balances utilization and exploration, where the largest selected action value
293 function is used, and other non-optimal actions still have a probability of being searched. The
294 ε -greedy strategy can be expressed by formula (24), where ε is the greedy rate and r is a random
295 number between 0 and 1. When $\varepsilon \geq r$, the probabilities of crossover and mutation that maximizes Q
296 value are chosen, when $\varepsilon \leq r$, probabilities of crossover and mutation at random are chosen.

297
$$\pi(s_t, a_t) = \begin{cases} \max_a Q(s_t, a_t), & \varepsilon \geq r \\ \text{random value}, & \varepsilon < r \end{cases} \quad (24)$$

298 3.3. Design of GSAA-RL algorithm

299 This section describes the process of the Q-learning algorithm dynamically adjusting the
300 crossover probability P_c and mutation probability P_m in detail.

301 Crossover and mutation operations play an extremely important role in the genetic algorithm, and
302 the key parameters of crossover and mutation operations are P_c and P_m . In the iterative process
303 of the algorithm, if P_c and P_m are too large, the solution will converge too slowly and if the
304 values are too small, it will be difficult to generate new individuals [32]. However, reinforcement
305 learning has the advantage of being able to select the suitable parameters dynamically. Therefore,
306 reinforcement learning is introduced to adjust P_c and P_m , so that the solution effect can better meet
307 the actual situation.

308 It can be divided into four steps by reinforcement learning to adjust two main parameters in the
309 genetic algorithm. First, the agent obtains the state s_t of the time step t in the iterative process of
310 the genetic simulated annealing algorithm (line 5 in algorithm 1). Secondly, it performs the
311 corresponding action a_t according to the specified action selection strategy (line 6 in algorithm 1).
312 Then, it is followed by the genetic, repair, and simulated annealing operations (lines 9-13 in algorithm
313 1). At this time, the state of the genetic simulated annealing algorithm is shifted to s_{t+1} , and the
314 feedback is returned to the agent. Finally, the agent will conduct the action a_{t+1} . The agent records
315 the learning process according to the existing state, action, the feedback received and updates the Q
316 table at the same time (line 8 in algorithm 1). If the reward is positive, the action selection of the
317 genetic simulated annealing algorithm will be strengthened; if the reward is negative, it will be
318 weakened accordingly [31]. The process of continuously acquiring states, executing actions, obtaining
319 feedback, and adjusting strategies constitutes of the reinforcement process.

320 After several iterations, the reinforcement learning process is activated, and the selection of P_c
321 and P_m will be optimized based on the past and current learning experience.

322 Based on the above series of descriptions, the complete pseudo code of the GSAA-RL is shown
323 in **Algorithm 1**, and the flow chart of GSAA-RL algorithm is presented in Fig. 2.

Algorithm 1. GSAA-RL

GSAA-RL parameters: population size ($NIND$), maximum iteration number ($MAXGEN$), probability
of selection operation ($GGAP$), Q table, state set (S), action set (A).

Input: Pop_{init} ($t = 0$)

1: $F_t \leftarrow$ fitness value calculation for the current time step

2: $a_t, s_t \leftarrow$ choose action and state randomly

3: **While** $t < MAXGEN$ **do**

4: $F_{t+1} \leftarrow$ fitness value calculation

5: $s_{t+1} \leftarrow$ calculate the state of GSAA-RL according to Eq.(19)

6: $a_{t+1} \leftarrow$ choose action according to $\varepsilon - greedy$

7: $r_{t+1} \leftarrow$ calculate reward value for the next time step according to Eqs.(22-23)

8: $Q(s_{t+1}, a_{t+1}) \leftarrow$ update Q table according to Eq.(18)

9: $Pop_{t+1} \leftarrow$ selection operation

10: $Pop_{t+1} \leftarrow$ crossover operation

11: $Pop_{t+1} \leftarrow$ mutation operation

12: $Pop_{t+1} \leftarrow$ repair operation

13: $Pop_{t+1} \leftarrow$ simulated annealing operation

14: $t \leftarrow t + 1$

15: End while

Output: Optimal schedule sequence

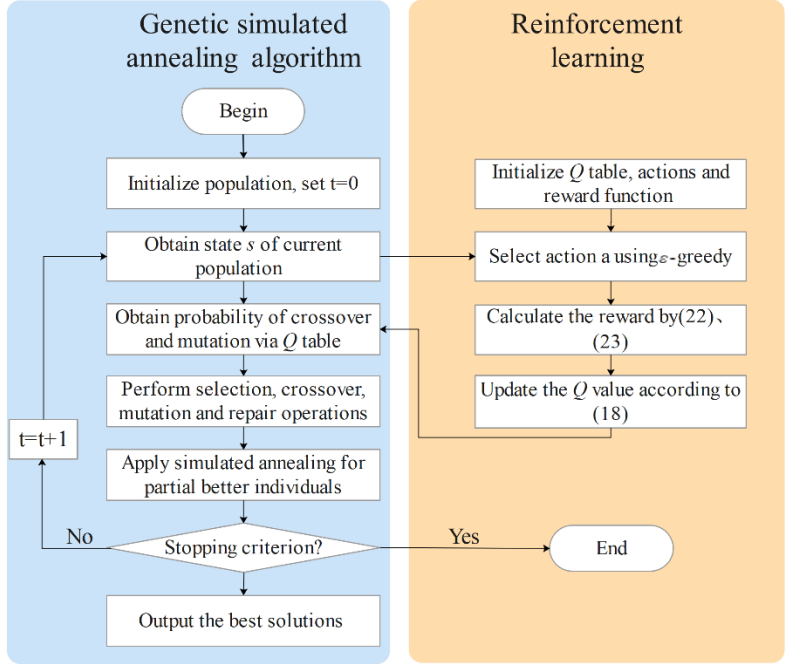


Fig. 2. Flow chart of the GSAA-RL algorithm

4. Computational experiments based on real cases

In this section, computational experiments are given to validate the effectiveness of the proposed model and solution algorithm using the field survey data of Comprehensive Port in Huanghua. Fig. 3. is the sketch of Comprehensive Port in Huanghua, with a 200,000 ton one-way narrow and long channel with a total length of 31 nautical miles. In particular, because of the limit of channel depth, ships with a draft of more than 18m and a length of more than 280m must take the tide to enter the port. Due to a large number of ore importers and small batches, in addition to 200,000 ton ships entering and leaving the port every day, 50,000-100,000 ton ships also occupy a certain proportion, which will cause port detention to a certain extent. Therefore, it is significantly important to find a feasible dispatching plan for ships entering and leaving the port to alleviate the congestion phenomenon. There are 8 anchorages and 15 berths in the Comprehensive Port in Huanghua. For the convenience of calculation, the anchorage numbers are marked as 1-8, and the berth numbers are marked as 1-15. The detailed information for the berth, anchorage of Comprehensive Port in Huanghua is presented in Appendix A. The scope of the numerical experiments also included a detailed evaluation of the convergence patterns and boxplot for the considered solution algorithms, which can be found in Appendix B.

There are two groups of instances used in this paper. The first group with different number of ships (6-35 ships for small-scale instances as well as 42-83 ships for large-scale instances) are considered to examine the efficiency of the proposed algorithm with GA, GSAA, CPLEX, the instances of 35 ships can be expressed as V35. The second group with different number of ships (5-80 ships) is used to compare the GSAA-RL with the real port scheduling scheme (FCFS). All experiments are conducted on a computer with a CPU of 3.5 GHz, RAM size of 64 GB, and running version 12.6.



Fig. 3. The sketch of Comprehensive Port in Huanghua

348

349

350 4.2 Benchmark methods

351 To evaluate the performance of the proposed GSAA-RL algorithm, four benchmark methods are
 352 introduced to solve the MILP model and compared with our algorithm. The first benchmark method
 353 is the CPLEX solver, and the maximum computational time is set to the 3600s. The second benchmark
 354 method is the First-Come-First-Served (FCFS) strategy simulating the decision of a VTS operator,
 355 which is commonly used in ports at present. The other two methods are heuristic algorithms, namely
 356 genetic algorithm (GA) and genetic simulated annealing algorithm (GSAA).

357 4.3 Parameter settings

358 The developed GSAA-RL algorithm will be compared with 4 state-of-the-art methods (i.e.,
 359 CPLEX solver, FCFS strategy, GA algorithm, and GSAA method), which have been frequently used
 360 in ship scheduling literature. Each of the considered algorithms has a set of parameters, which remain
 361 constant during the search progress. The parameters related to the GSAA-RL algorithm are set as
 362 follows: learning rate $\alpha = 0.6$, discount rate $\gamma = 0.65$, greedy rate $\varepsilon = 0.5$, crossover and mutation
 363 probabilities are adjusted dynamically according to Q-learning, and initial Q value are all 0. The
 364 parameters related to the GA and GSAA algorithms are set as follows: the maximum number of
 365 iterations $MAXGEN = 400$, the number of population $NIND = 200$, selection probability
 366 $GGAP = 0.9$, initial temperature $T_0 = 2$, cooling factor $\alpha_1 = 0.9$, crossover probability $Pc = 0.85$,
 367 mutation probability $Pm = 0.21$. The other parameters are set as follows: same-direction safety
 368 clearance $g_1 = 5$, different-direction safety clearance $g_2 = 5$. Each instance is run for 10 times.

369 4.4. Experimental results and analysis of 13 ships

370 In this subsection, the proposed model and algorithm are tested using the 13 ships in the
 371 Comprehensive Port in Huanghua on a certain day in May 2021. The basic data of 13 ships includes
 372 the direction of the ship entering and leaving the port, ship speed, berth ID, and anchorage ID, etc., as
 373 shown in Table 6. Table 7 reports the optimal scheduling scheme of the 13 ships solved by the proposed
 374 GSAA-RL algorithm. From the results shown in Table 7, it is revealed that the sequence of ships
 375 entering and leaving the port, the navigation continuity of all ships, and the time when the ships
 376 approach the channel, leave the channel and reach the berth, respectively. At the same time, it can be
 377 observed that the first ship scheduled is inbound no.1, its scheduling start time is at 0 min, and the last

378 ship to leave the channel is inbound no.13 at 957 min. Table 8 is the chromosome with the shortest
 379 total time spent by the 13 ships entering and leaving the port. It is also clear that the optimal scheduling
 380 scheme and navigation direction of all ships by reading this chromosome from Table 8, for example,
 381 121 indicates that ship no.12 in the state entering the port and the ranking is 8. To further show the
 382 scheduling results of the 13 ships in Table 8, the Gantt chart is drawn in Fig. 4. From Fig. 4, we better
 383 visualize the waiting time, sailing time, sailing direction of each ship.

384 The evolution process of parameters Pc and Pm is presented in Fig. 5. As shown in Fig. 5, in the
 385 initial and intermediate stages of the algorithm, Pc and Pm almost change between large and small
 386 values. After the rapid convergence of two phases, Pc and Pm only evolve within a small range. It
 387 can be observed that Pc and Pm are constantly searching for optimization until the objective value
 388 reaches the minimum. The experimental results of comparing the unimproved and new reward
 389 functions are shown in Fig. 6. Reward function 2 represents the convergence result of GSAA-RL
 390 without improving the reward function. The minimum total time spent by entering and leaving the port
 391 is found around 180 generations, and it is 2615min. Reward function 1 represents the convergence
 392 result of GSAA-RL with an improved segmented reward function, it can be obtained that after around
 393 170 generations, the minimum total time of entering and leaving the port is found and the total time is
 394 2546min. It is obvious that new segmented reward function 1 can improve the learning efficiency of
 395 Q-learning and reduces the number of GSAA-RL algorithm iteration.

96 **Table 6**

97 Data of 13 ships.

NO.	IO	Berth ID	Anchorage ID	Ship length (m)	Ship width (m)	Ship speed (kn)	Application time (min)	Ship draft (m)	Tidal time window(min)
1	1	13	2	225	32	13.65	0	10.35/10.75	
2	0	13	-	225	37	11.24	90	13/13.1	
3	0	5	-	292	45	14.24	153	6.36/8.7	
4	0	4	-	240	38	7.4	185	5.17/7.12	
5	1	5	5	229	32	13.65	225	12.88/12	
6	1	2	2	150	21	9.25	275	8.7	
7	1	4	3	190	32	12.12	302	12.88/13.13	
8	0	6	-	289	45	11.6	356	13.5/13.5	
9	0	7	-	295	46	9.01	396	6.5/8.6	
10	0	15	-	157	21	7.7	425	8.3	
11	1	6	2	292	45	12.31	470	18.10/18.22	[540,750]
12	1	15	6	122	21	8.48	493	6	
13	1	7	2	325	57	12.97	560	11.38/12.5	

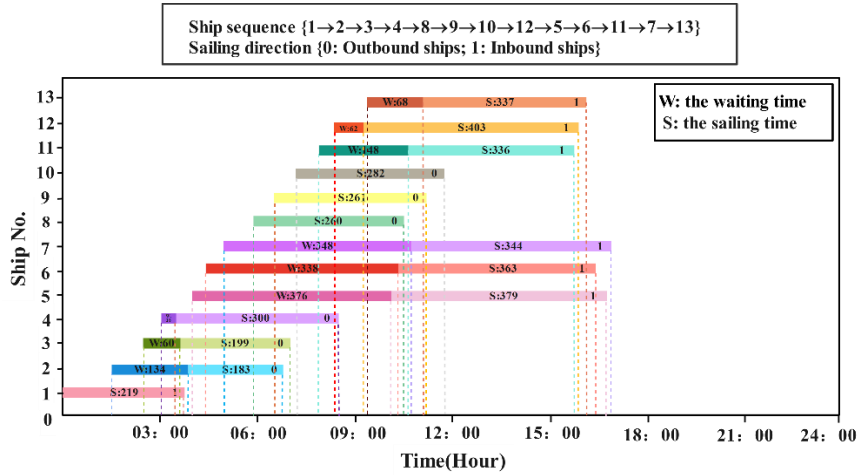


Fig. 4. Gantt diagram of the optimization result of 13 ships experiments

Table 7

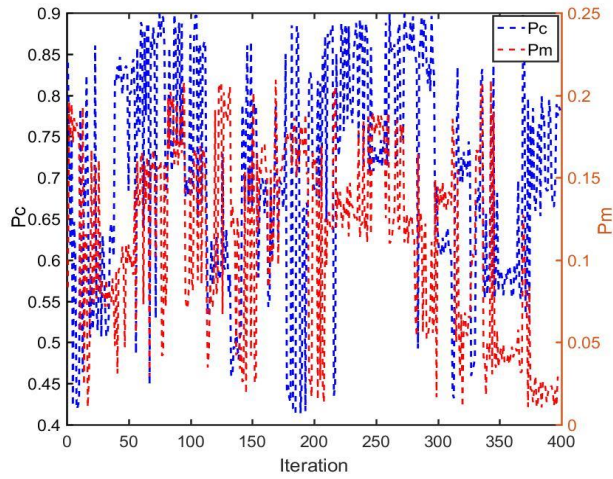
Optimal results of 13 ships experiments using GSAA-RL algorithm.

No.	IO	Average speed (kn)	Adjusted average speed (kn)	Application time (min)	Begin scheduling time (min)	Approach channel time (min)	Leave channel time (min)
1	1	13.65	13.65	0	0	68	205
2	0	11.24	11.24	90	224	241	407
3	0	14.24	11.24	153	213	246	412
4	0	7.4	7.4	185	203	251	503
8	0	11.6	7.4	356	356	364	616
9	0	9.01	7.4	396	396	405	657
10	0	7.7	7.4	425	425	455	707
12	1	8.48	8.48	493	555	712	932
5	1	13.65	8.48	225	601	717	937
6	1	9.25	8.48	275	613	722	942
11	1	12.31	8.48	470	618	727	947
7	1	12.12	8.48	302	650	732	952
13	1	12.97	8.48	560	628	737	957

Table 8

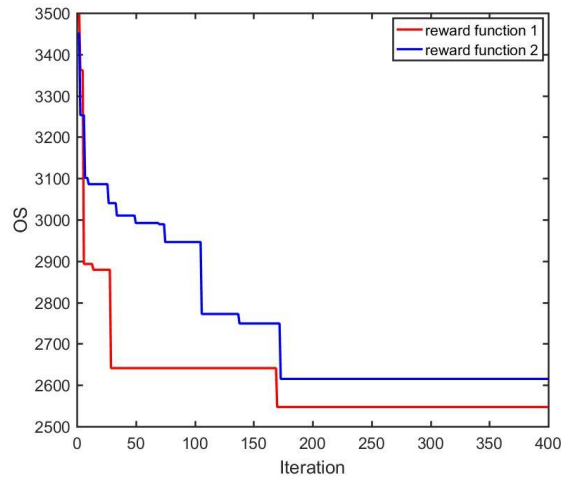
Chromosome with the shortest total time spent by ships entering and leaving the port.

11	20	30	40	80	90	10	121	51	61	111	71	131
----	----	----	----	----	----	----	-----	----	----	-----	----	-----



406
407

Fig. 5. The evolution process of parameter P_c and P_m .



408
409

Fig. 6. Comparison of the optimization process with unimproved and of new reward functions.

410 *4.5. The verification of the model rationality with the case of the 13 ships*

411 The rationality of the model can be verified from the perspective of constraints such as ship speed
 412 adjustment, tidal time window, safe clearance between the same and different direction ships, and
 413 navigation continuity in Table 7. Speed adjustment is to adjust the speed of ships successively in the
 414 same direction to avoid overtaking on the channel. For example, the outbound ship no.8 follows the
 415 outbound ship no.4 on the channel. The speed of ship no.8 cannot exceed that of ship no.4, which
 416 should be adjusted from 11.6kn to 7.4kn. In addition, ships can only be dispatched after they apply for
 417 entry and exit. With reference to this rule, an illustrative example is that only after the outbound ship
 418 no.4 approaches the channel, a safe clearance later, the outbound ship no.8 can approach the channel.
 419 However, the outbound ship no.8 has not applied for leaving the port at this time. Consequently, the
 420 outbound ship no.8 cannot be arranged to leave the port until the application is made at 356min. The
 421 inbound ship no.11 completes entering the port within the time window [540,750], meeting the
 422 constraint of the tidal time windows.

423 *4.6. Effectiveness of the proposed GSAA-RL algorithm*

424 *4.6.1 Comparison of the results of the GSAA-RL with CPLEX and GSAA, GA*

425 In this subsection, we first solve the MILP described in Section 2.2 using the proposed GSAA-
426 RL algorithm and three benchmark methods, namely GSAA, GA, and CPLEX methods. We set the
427 same parameters for all five methods, for example, $g_1 = 5, g_2 = 5$. We compare the results of GSAA-
428 RL with GSAA, GA, and CPLEX in terms of the total time spent by ships entering and leaving the
429 port, and the computational efficiency under different scale instances. All scale instances in the
430 experiment are generated from the Comprehensive Port in Huanghua, each instance is run for 10 times.
431 Table 9 and 10 presents the computational results of the proposed GSAA-RL, GA, GSAA, and CPLEX
432 methods for small-scale and large-scale instances respectively, where the notation “OS_{IP}”, “OS_{GA}”,
433 “OS_{GSAA}”, “OS_{GSAA-RL}” denote the objective values of the MILP, the optimal solution generated by
434 the GA algorithm, GSAA algorithm, and the GSAA-RL, respectively.
435

36
37
38
39 **Table 9**
40 Computational results for the small-scale instances.

Instance	CPLEX		GA		GSAA		GSAA-RL		Gap1(%)	Gap2(%)
	CPU(s)	OS _{IP}	CPU(s)	OS _{GA}	CPU(s)	OS _{GSAA}	CPU(s)	OS _{GSAA-RL}		
V6	6.72	1261	9.04	1288	25.75	1261	26.89	1261	2.10	0
V10	33.14	2038	13.37	2674	37.56	2071	39.22	2038	23.78	1.59
V13	665.12	2546	17.01	2867	49.07	2607	49.54	2546	11.20	2.34
V18	1534.23	3908	23.88	4234	56.89	4177	62.97	3722	12.09	10.89
V23	3245.21	5220	64.34	7385	82.16	6840	83.24	6649	9.97	2.79
V28	3600.00	-	85.25	13208	106.22	12054	107.25	11806	7.00	5.54
V35	3600.00	-	47.18	15442	161.27	15337	169.90	13508	12.52	11.93
Average	1812.06	-	37.01	6730	74.13	6335	77.00	5933	11.24	5.01

41 Notes: Gap1=(OS_{GA} - OS_{GSAA-RL})/OS_{GA} × 100%; Gap2=(OS_{GSAA} - OS_{GSAA-RL})/OS_{GSAA} × 100%;

442 It becomes obvious that compared with the GSAA-RL, the CPLEX is faster only when solving
443 the instances with 6, 10, 13, 18 ships. The computational time of the CPLEX in solving NILP shows
444 an exponential growth with the increase of the instance scale. In particular, CPLEX cannot even obtain
445 any feasible solution for some large-scale instances with 63, 68, 73, 78, 83 ships due to the complexity
446 of the problem. Therefore, such a solution method cannot meet the actual needs of the port. The GA
447 and GSAA-RL algorithms can obtain a feasible solution under the one-hour time limit, but the quality
448 of the solutions is relatively poor for the small-scale and large-scale instance. This is because the
449 solution is obtained by fixing the values of key parameters in each iteration, thus leading to faster
450 convergence. In contrast to these two methods, the solutions obtained by the GSAA-RL are not inferior
451 to the solutions obtained by the GA and GSAA, and the advantage of the GSAA-RL becomes more
452 remarkable with the increase of the instance scale. The solution obtained by GSAA-RL is 11.24% and
453 5.01% better than that of the GA and GSAA for small-scale instances, and 18.58% and 11.58% for
454 large-scale instances, reflecting the superiority of the proposed algorithm. Concerning the time
455 consumption, relatively higher computation time is recorded in GSAA-RL compared to that of GSAA,
456 because the additional time is required to reselect the crossover and mutation probability values from
457 the Q table to complete the evolution operations in each iteration in order to expand the search scope.
458 However, the maximum GSAA-RL computational time did not exceed 15.75min (83 ships). Therefore,

459 the port operators will be able to develop and revise ship scheduling plans in a timely manner. Based
 460 on the conducted computational experiments, the developed GSAA-RL algorithm outperformed the
 461 CPLEX solver, GA, and GSAA algorithms, demonstrating the effectiveness of the proposed algorithm.

462 *4.6.2 Comparison of the results of the GSAA-RL and the real port scheduling schemes.*

463 To validate the effectiveness of the model, the scheme provided by the GSAA-RL is compared
 464 to the real port scheduling schemes. According to the field surveys of Comprehensive Port in
 465 Huanghua, the real port scheduling scheme mainly adopts a FCFS rule for ship scheduling.
 466 Specifically, it arranges ships to enter and leave the port successively according to the application time
 467 of ships and preferentially assigns tide-dependent ships in the tidal time windows.

468 Table 11 shows the comparison among the results of the proposed scheme and the FCFS
 469 scheduling scheme. It is found that for all instances, the GSAA-RL is constantly better than the FCFS
 470 scheme, and the average gap arrives at 46.04%. It is because the order of ships has been determined
 471 in the FCFS strategy in advance, and it is difficult to arrange a reasonable scheduling order. This result
 472 indicates that the proposed model can significantly help port operators to reduce the total time spent
 473 by ships in port, thus achieving higher throughput and better emission performance.

474

75 **Table 10**

76 Computational results for the large-scale instances.

Instance	CPLEX		GA		GSAA		GSAA-RL		Gap1(%)	Gap2(%)
	CPU(s)	OS _{IP}	CPU(s)	OS _{GA}	CPU(s)	OS _{GSAA}	CPU(s)	OS _{GSAA-RL}		
V42	3600	-	62.06	25479	219.96	22176	233.41	20410	19.89	7.77
V48	3600	-	79.85	33234	272.78	32314	281.40	28454	14.38	11.95
V55	3600	-	195.25	41095	367.55	39125	377.10	36135	12.07	7.67
V63	3600	-	249.71	49283	452.32	48188	455.19	47381	3.86	1.67
V68	3600	-	305.88	68996	510.93	58417	526.71	52737	23.57	9.72
V73	3600	-	420.66	83429	660.42	80082	672.13	67574	19.00	15.62
V78	3600	-	506.07	128196	723.44	112967	735.27	85254	33.50	24.53
V83	3600	-	745.45	138458	856.23	124584	945.12	107545	22.33	13.68
Average	3600	-	320.62	71021	507.95	64731	528.29	55686	18.58	11.58

478

479 **5. Conclusion and scope of future work**

480 The rapid development of ships tonnage has caused great challenges on the capacities of ports,
 481 leading to frequent ship delays and heavy port congestion. Thus, effective ship scheduling scheme is
 482 required to cope with the phenomenon. This article presents an MILP mathematical model for the ship
 483 schedule problem with minimizing the total time spent by ships in port. The novel GSAA-RL
 484 algorithm is designed to solve the MILP model. In the proposed GSAA-RL, the genetic algorithm is
 485 considered as the basic optimization algorithm, and Q-learning with a unique property of selecting
 486 suitable parameters dynamically is developed to adjust the parameters of crossover and mutation to
 487 improve the search ability of the algorithm. In addition, given the fact that the genetic algorithm may
 488 fall into local optimum, a simulated annealing operation is implemented to some excellent individuals
 489 after genetic operations to further enhance the search ability of solution space.

490 To verify the effectiveness of the proposed GSAA-RL algorithm, taking the data of
491 Comprehensive Port in Huanghua as an example, we compare the computational results of the
492 proposed solution algorithm in this paper with those of a MILP/CPLEX solver, a FCFS strategy, a GA
493 method, and a GSAA algorithm. Computational experiments demonstrate that the GSAA-RL
494 algorithm proposed significantly outperforms three existing methods (i.e., the CPLEX, GA, and
495 GSAA) in terms of solution quality when solving the small-scale and large-scale instances. In contrast
496 to the real port scheduling schemes (i.e., FCFS strategy), the scheme obtained by the proposed GSAA-
497 RL algorithm can reduce the total time spent by ships entering and leaving the port by an average of
498 43.91%. These computational performances highlight the effectiveness of the proposed solution
499 algorithm in the practical applications. The algorithm proposed in this paper provides a new tool for
500 ship traffic scheduling and makes up for the shortcomings of some existing scheduling optimization
501 methods.

502 Current research can be expanded from the following two aspects. First of all, from the
503 perspective of the model, taking into account the actual situation, some input parameters (such as the

504 **Table 11**

505 Comparison of the results of the GSAA-RL and the real port scheduling schemes.

Instance	FCFS		GSAA-RL		Gap(%)
	CPU(s)	OS _{FCFS}	CPU(s)	OS _{GSAA-RL}	
V5	0.34	1095	25.30	1078	1.55
V9	0.35	2362	37.98	1910	19.14
V15	0.35	5490	58.80	3317	39.58
V20	0.35	9478	77.65	5784	38.97
V25	0.39	15026	100.47	8597	42.79
V30	0.38	21460	124.03	11037	48.57
V36	0.39	30846	173.18	13950	54.78
V43	0.37	44134	231.63	22906	48.10
V49	0.39	58919	295.71	28829	51.07
V54	0.36	75304	355.24	31001	58.83
V60	0.39	98214	423.92	39117	60.17
V65	0.37	119935	468.75	46345	61.36
V70	0.38	142863	548.05	55727	60.99
V75	0.36	167731	636.11	75478	55.00
V80	0.38	195503	821.45	98452	49.64
Average	0.37	65891	291.88	29569	46.04

506 Notes: $\text{Gap} = (\text{OS}_{\text{FCFS}} - \text{OS}_{\text{GSAA-RL}}) / \text{OS}_{\text{FCFS}} \times 100\%$;

507 ship's expected arrival time) may be affected by the weather and its own mechanical failure, which
508 may cause the arrival time to be uncertain and affect the initial ship scheduling plan. Therefore, the
509 ship scheduling problem under the uncertain conditions has practical significance, and this part is
510 being studied as a key content of the authors' current work and will be presented in a separate cover
511 in the future. Secondly, from the perspective of algorithm applications, the GA-RL algorithm can be
512 applied to the optimization problem of ship scheduling in two-way, compound and restricted channels,
513 in order to shorten the total waiting time of ships in port and improve the efficiency of channel
514 navigation. Finally, methodologically, use of reinforcement learning to adjust the key parameters of
515 other optimization algorithms, such as tabu search algorithm, particle swarm optimization algorithm,

516 can be further investigated to improve the search performance of the algorithm.

517 **CRedit authorship contribution statement**

518 **Runfo Li:** Conceptualization, Methodology, Data curation, Software, Writing – original draft,
519 Writing – review & editing. **Xinyu Zhang:** Conceptualization, Supervision, Project administration,
520 Funding acquisition, Writing – review & editing, Validation. **Lingling Jiang:** Conceptualization,
521 Methodology, Investigation, Writing – review & editing. **Wenqiang Guo:** Conceptualization,
522 Methodology, Writing – review & editing.

523 **Declaration of Competing Interest**

524 The authors declare that they have no known competing financial interests or personal
525 relationships that could have appeared to influence the work reported in this paper.

526 **Acknowledgments**

527 This work was financially supported by the Central Guidance on Local Science and Technology
528 Development Fund of Shenzhen (grant no.2021Szvup014), and the National Natural Science
529 Foundation of China (grant no. 51779028). The authors thank the referees for helpful comments and
530 suggestions.

531 **Appendix A: berth, and anchorage information for Comprehensive port in Huanghua**

532 The length of the planning horizon in this paper is set to 2 days for small-scale instances (6-35
533 ships) and 3 days for large-scale instances (42-83 ships) to show the applicability of the model. We set
534 both the safe navigation distance and the unit of the time step to 10 minutes. Table A1 records the
535 distance between the anchorage and buoy no.201, and the distance between the berth and the buoy
536 no.262 is depicted in Table A2.

537 **Table A1**

538 Distance between the anchorage and the buoy no.201.

Anchorage ID	Distance(nm)
1	15.472
2	15.396
3	11.459
4	16.381
5	16.256
6	22.111
7	17.123
8	10.39

539 **Table A2**

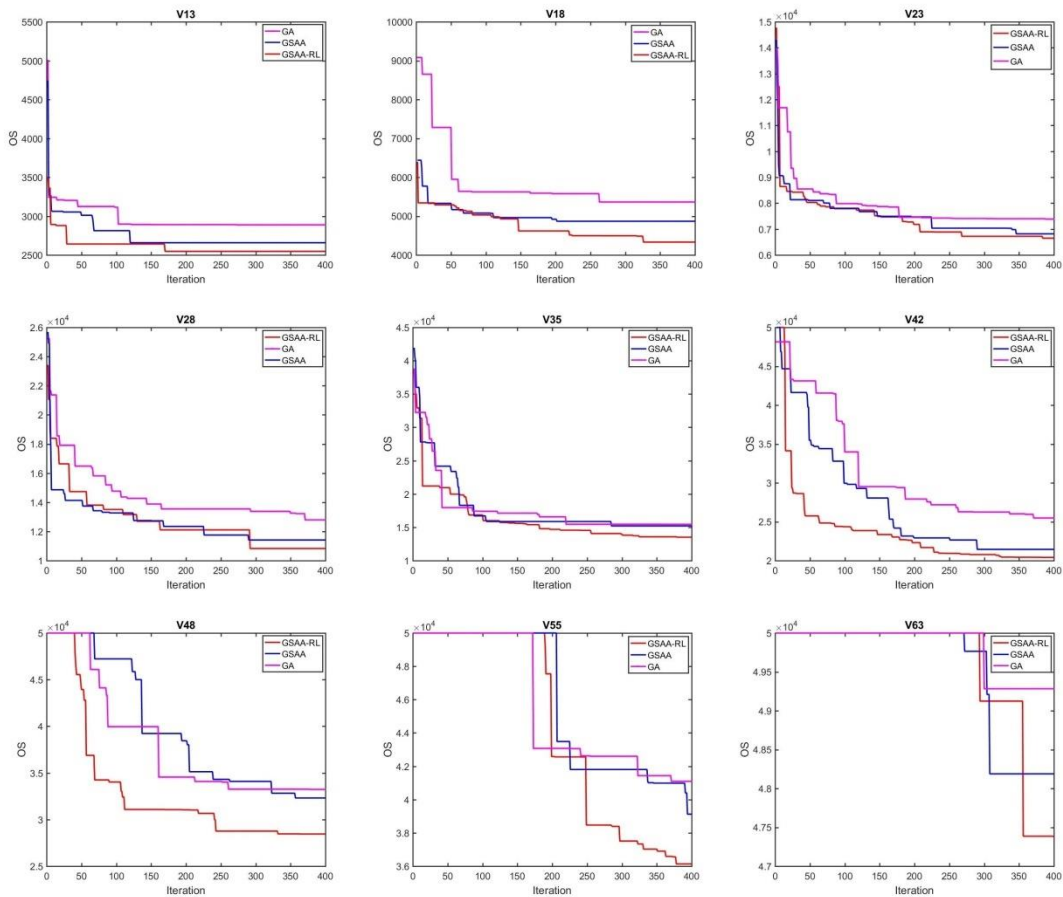
540 Distance between the berth and the buoy no.262.

Berth	Berth ID	Distance(nm)	Berth	Berth ID	Distance(nm)
HG1	1	4.691	GC2	9	1.159
HG2	2	4.798	GC3	10	2.372
HG3	3	5.617	GC4	11	3.337
HG4	4	5.845	GC5	12	2.893
HG5	5	6.002	GC6	13	3.164

K01	6	0.914	GC7	14	3.395
K02	7	1.083	GC8	15	3.622
GC1	8	1.035	-	-	-

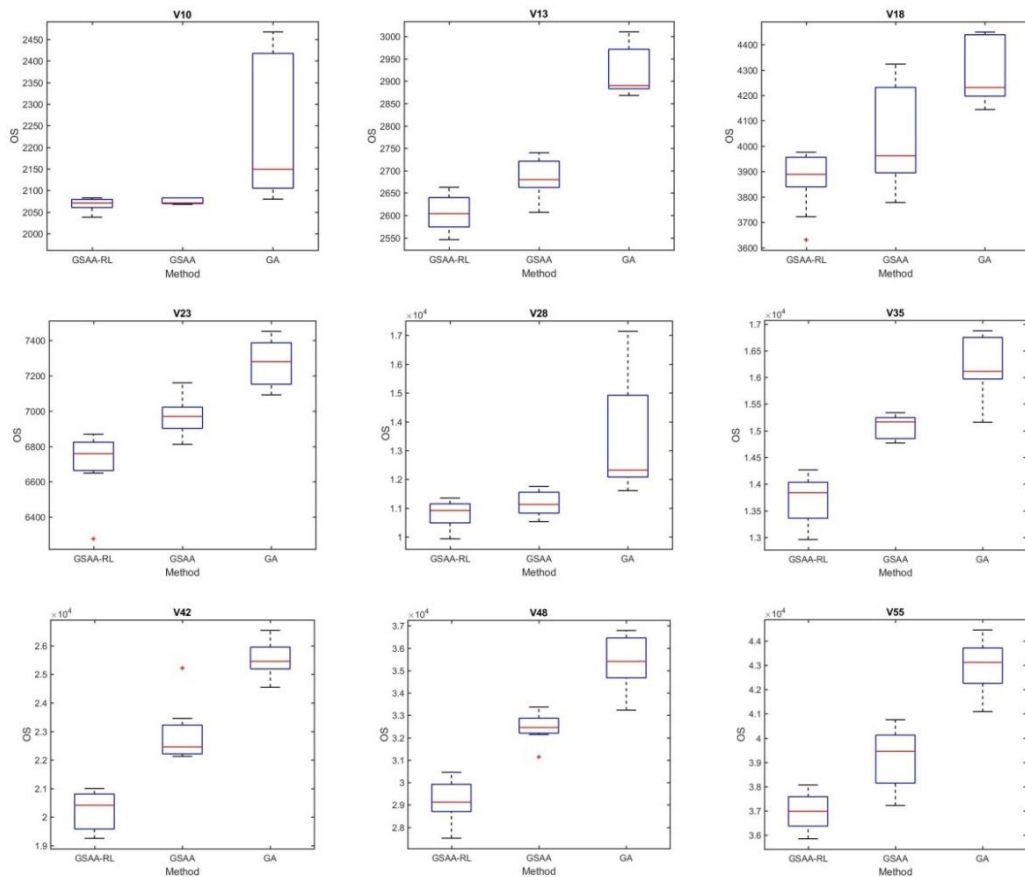
541 **Appendix B: convergence curve and boxplot comparison for different algorithms**

542 The analysis of convergence patterns allows keeping track of the objective function value
543 improvements from one generation to another (in case of the considered GA, GSAA, GSAA-RL). The
544 convergence patterns were shown only for the some small-scale and large-small instances [V13, V18,
545 V23, V28, V35, V42, V48, V55, V63] and presented in Fig. 7. Based on the convergence pattern
546 analysis, it can be noticed that GSAA-RL was able to identify the promising solutions of the search
547 space much faster as compared to the GA, and GSAA algorithms, and allows effective exploration of
548 the search space and identification of the domains with high-quality solutions. Besides, the boxplot
549 figure of OS value (i.e., the total time spent by ships in port) from GA, GSAA, GSAA-RL is shown in
550 Fig. 8 for the some small-scale and large-small instances [V10, V13, V18, V23, V28, V35, V42, V48,
551 V55], which could further validate the effectiveness of the GSAA-RL algorithm. It can be observed
552 from Fig. 8 that the OS values obtained by GSAA-RL algorithm have smaller median and range, which
553 further illustrates the effectiveness of the proposed GSAA-RL in this paper for solving the ship
554 scheduling problem.



555

556 **Fig. 7.** The convergence curves of different algorithms for small-scale and large-scale instances
557 [V13, V18, V23, V28, V35, V42, V48, V55, V63].



558

559 **Fig. 8.** The boxplot of three algorithms for for small-scale and large-scale instances [V10, V13, V18,
560 V23, V28, V35, V42, V48, V55].

561 Reference

- 562 [1] UNCTAD. Review of maritime transport, 2017. United Nations Conference on Trade and
563 Development.
- 564 [2] Jia S, Li CL, Xu Z, 2019. Managing navigation channel traffic and anchorage area utilization of
565 a container port. *J. Transportation Science*. 53(3):728-745.
- 566 [3] Wu YQ, Zhang R, 2021. Integrated optimization of continuous berth allocation and ship
567 dispatching under one-way channel. *J. Computer Engineering and Applications*.
- 568 [4] Liu BL, Li ZC, Wang YD, Sheng DA. 2021 Short-term berth planning and ship scheduling for a
569 busy seaport with channel restrictions. *J. Transportation Research Part E* .154.
- 570 [5] Li SQ, Jia S, 2019. The seaport traffic scheduling problem: Formulations and a column-row
571 generation algorithm. *J. Transportation Research Part B*. 128:158-184.
- 572 [6] Zhang XY, Lin J, Guo ZJ, Liu TS, 2016. Vessel transportation scheduling optimization based on
573 channel-berth coordination. *J. Ocean Engineering*. 112:145-152.
- 574 [7] Lalla-Ruiz E, Shi XN, Voß SX, 2018. The waterway ship scheduling problem. *J. Transportation
575 Research Part D*. 60:191-209.
- 576 [8] Pei YL, Chen DJ, 2018. Study on the optimal dispatching algorithm of ships in and out of tidal
577 two-way channel. *C. IEEE 4th Information Technology and Mechatronics Engineering
578 Conference. IEEE*. 324-329.

- 579 [9] Zheng HX, Liu BL, Deng CY, Feng PP, 2018. Ship scheduling optimization in one-way channel
580 bulk harbor. *J. Operations Research and Management Science*. 27(12):28-37.
- 581 [10] Meisel F, Fagerholt K, 2019. Scheduling two-way ship traffic for the Kiel Canal: Model,
582 extensions and a matheuristic. *J. Computers & Operations Research*. 106:119-132.
- 583 [11] Soroush FA, Reza TM, Dorsa A, Behdin VN, 2020. Simultaneous waterway scheduling, berth
584 allocation, and quay crane assignment: A novel matheuristic approach. *J. International Journal of*
585 *Production Research*.
- 586 [12] Andersen T, Hove JH, Fagerholt K, Meisel F, 2021. Scheduling ships with uncertain arrival times
587 through the Kiel Canal. *J. Maritime Transport Research*. 2.
- 588 [13] Zhang XY, Li RJ, Lin J, Xu CB, 2018. Optimization modeling of vessel traffic scheduling for Y
589 shaped bifurcated compound waterway. *J. Journal of Dalian Maritime University*. 44(2):1-14.
- 590 [14] Zhang XY, Li RJ, Lin J, Chen X, 2018. Vessel scheduling optimization in two-way traffic ports.
591 *J. Navigation of China*. 41(2):36-40.
- 592 [15] Liu BL, L ZC, Sheng D, Wang YD, 2021. Integrated planning of berth allocation and vessel
593 sequencing in a seaport with one-way navigation channel. *J. Transportation Research Part B*.
594 143:23-47.
- 595 [16] Zhang B, Zheng ZY, Wang DQ, 2020. A model and algorithm for vessel scheduling through a
596 two-way tidal channel. *J. Maritime Policy & Management*. 47(2):188-202.
- 597 [17] Liu DD, Shi GY, Hirayama K, 2021. Vessel scheduling optimization model based on variable
598 speed in a seaport with one-way navigation channel. *J. Sensors*. 21(16):5478.
- 599 [18] Zhang XY, Chen X, Ji MJ, Yao S, 2017. Vessel scheduling model of a one-way port channel. *J.*
600 *Journal of Waterway Port Coastal & Ocean Engineering*. 143(5):04017009.
- 601 [19] Li JJ, Zhang XY, Yang BD, Wang NN, 2020. Vessel traffic scheduling optimization for restricted
602 channel in ports. *J. Computers & Industrial Engineering*. 152(3):107014.
- 603 [20] Zhao J, Liu SX, Zhou MC, Guo XW, Qi L, 2018. Modified cuckoo search algorithm to solve
604 economic power dispatch optimization problems. *J. IEEE-CAA Journal of Automatic Sinica*.
605 5(4):794-806.
- 606 [21] Zhang YW, Wang L, Wu QD, 2014. Dynamic adaptation cuckoo search algorithm. *J. Control*
607 *Decision*. 29(4):617-622.
- 608 [22] Shahrabi J, Adibi MA, Masoud M, 2017. A reinforcement learning approach to parameter
609 estimation in dynamic job shop scheduling. *J. Computers & Industrial Engineering*. 110:75-82.
- 610 [23] Cao ZC, Lin CR, Zhou MC, 2021. A knowledge-based cuckoo search algorithm to schedule a
611 flexible job shop with sequencing flexibility. *J. IEEE Transactions on Automation Science and*
612 *Engineering*. 18(1):56-69.
- 613 [24] Pettinger JE, Everson RM, 2002. Controlling genetic algorithms with reinforcement learning. *C.*
614 *Proceedings of the 4th Annual Conference on Genetic and Evolutionary Computation*.
- 615 [25] Chen Y, Hu JL, Hirasawa K, Yu SN, 2007. Optimizing reserve size in genetic algorithms with
616 reserve selection using reinforcement learning. *C. Proceedings of Sice Annual Conference*. 1-8.
- 617 [26] Meng SS, Zhu Q, Xia F, Lu JF, 2020. Research on parameter optimization of dynamic priority
618 scheduling algorithm based on improved reinforcement learning. *J. IET Generation,*
619 *Transmission & Distribution*. 14(16):3171-3178.
- 620 [27] Fang YL, Ming H, Li MQ, Liu Q, Pham DT, 2019. Multi-objective evolutionary simulated
621 annealing optimization for mixed-model multi-robotic disassembly line balancing with interval
622 processing time. *J. International Journal of Production Research*. 58(3):846-862.

- 623 [28] Xue BP, Berseth G, Michiel VDP, 2016. Terrain-adaptive locomotion skills using deep
624 reinforcement learning. *J. Acm Transactions on Graphics*. 35(4):1-12.
- 625 [29] Chen RH, Yang B, Li S, Wang SL, 2020. A Self-learning genetic algorithm based on
626 reinforcement learning for flexible job-shop scheduling problem. *J. Computers & Industrial*
627 *Engineering*. 149.
- 628 [30] Bellman R, 1957. Dynamic programming and lagrange multipliers. *C. Proceedings of the*
629 *National Academy of Sciences of the United States of America*. 42:767-769.
- 630 [31] Emary E, Zawbaa HM, Grosan C, 2018. Experienced gray wolf optimization through
631 reinforcement learning and neural networks. *J. IEEE Transactions on Neural Networks and*
632 *Learning Systems*. 29:681-694.
- 633 [32] Bashir MB, Nadeem A, 2017. Improved genetic algorithm to reduce mutation testing cost. *J.*
634 *IEEE Access*. 5:3657-3674.